Electronic structure of wurtzite II-VI compound semiconductor cleavage surfaces studied by scanning tunneling microscopy

B. Siemens, C. Domke, Ph. Ebert, and K. Urban
Institut für Festkörperforschung, Forschungszentrum Jülich GmbH, 52425 Jülich, Germany
(Received 17 June 1997)

We report atomically resolved scanning tunneling microscopy (STM) images of cleavage surfaces of wurtzite II-VI compound semiconductors. CdSe(1120), CdSe(1010), and CdS(1010) were investigated. The STM images confirm a 1×1 reconstruction for all surfaces. At negative and positive sample voltages the occupied and empty dangling-bond states above anions and cations, respectively, dominate the contrast of the STM images. No states in the band gap were found. The electronic structure of the surface permits the observation of dopant atoms in subsurface layers and thus also cross-sectional scanning tunneling microscopy studies of point defects and heterostructures. [S0163-1829(97)04543-8]

I. INTRODUCTION

Scanning tunneling microscopy (STM) has recently evolved from a technique allowing atomic-scale investigations of surfaces into a powerful tool for studying bulk point defects and dopant atoms and correlating the defect concentrations with macroscopic properties of the materials.[1–4] The same technique, called cross-sectional scanning tunneling microscopy, has been used to study heterostructures as well.[5–10] The possibility of investigating defects is closely connected with the electronic and structural properties of the surfaces used for imaging the defects by STM. So far only cleavage surfaces of cubic III-V compound semiconductors have been suitable because of their favorable properties, which include (but are not limited to) a simple 1×1 reconstruction, one empty and one occupied dangling bond above each cation and anion, respectively, as well as, with the exception of GaP, the absence of surface states in the band gap. Recently, compound semiconductors with the hexagonal wurtzite structure have attracted growing attention because many promising materials for short-wavelength lasers occur only in the wurtzite structure. However, no atomically resolved STM investigation exists of cleavage surfaces of wurtzite compound semiconductors. Therefore, we investigated the electronic structure of nonpolar (1120) and (1010) cleavage surfaces of wurtzite CdSe and CdS by scanning tunneling microscopy and we discuss the possibility of bulk defect investigations on these surfaces by scanning tunneling microscopy.

II. EXPERIMENT

N-type CdSe and CdS single crystals grown by the Markov technique and doped with In (carrier concentrations of 7×10^{18} and 1×10^{19} cm^{-3}, respectively) were investigated. In order to cleave the crystals in ultrahigh vacuum (5×10^{-9} Pa) along the (1120) (for CdSe) and (1010) planes (for CdSe and CdS), we cut two slots into two opposite sides of the samples, which were oriented parallel to the normal vector of the desired cleavage plane. The samples were cleaved along the [0001] direction using a double-wedge cleavage technique. After cleavage, the crystals were immediately investigated by scanning tunneling microscopy without breaking the vacuum. Ohmic contacts were obtained by sputtering gold on two faces of the samples followed by an electrical discharge of a capacitor over these contacts. We used electrochemically etched tungsten tips.

III. RESULTS

The cleavage surfaces consist of typically 10-nm-wide flat terraces separated by steps. First we focus on the results obtained on the flat terraces of CdSe surfaces, but the same type of surface reconstruction was observed on CdS, as will be shown below. Figure 1 shows atomically resolved constant-current STM images of the occupied [frames (a1) and (b1)] and empty [frames (a2) and (b2)] density of states of the two nonpolar CdSe cleavage surfaces. For comparison the respective images obtained on the GaAs(110) surfaces are included in Figs. 1(c1) and 1(c2). The STM images of the (1120) surface [Figs. 1(a1) and 1(a2)] show zigzag chains along the [0001] direction in both the occupied and empty state images. These zigzag chains are separated from each other by 0.74 ± 0.05 nm. The periodic structure along the zigzag chain is repeated every 0.78 ± 0.05 nm. The surface unit cell of the CdSe(1120) surface is indicated in Fig. 1(a1). The width of the zigzag chain (measured perpendicular to the chain direction from the maxima on the left-hand side of the chain to those on the right-hand side of the chain) is 0.23 ± 0.01 nm.

The STM images of the CdSe($10\bar{1}0$) surface exhibit a rectangular pattern. The dimensions of the surface unit cell shown in Fig. 1(b1) are 0.43×0.70 nm^2 ($\pm5\%$). The longer side of the surface unit cell is oriented parallel to the [0001] direction. The surface unit cell of the (1120) surface is about 50% larger than that of the (1010) surface. We never observed any other surface reconstructions on either of the two surfaces (in more than 380 images covering approximately 0.3 μm^2 of surface area).

We did not observe any significant changes of the morphology on either surface if the tunneling voltage was changed, but the polarity maintained. No tunneling was possible for voltages between about -1.8 and $+1$ V. This indicates that no surface states exist in the band gap (1.8 eV

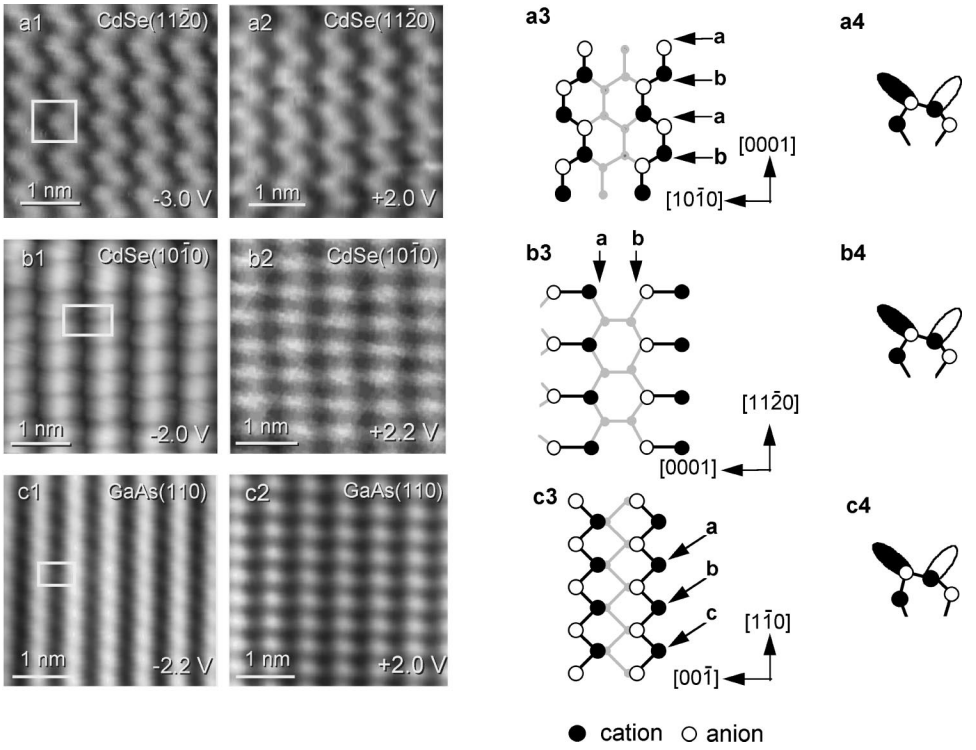

FIG. 1. Occupied (frames labeled 1, column on the extreme left) and empty (labeled 2, second column from left) state images as well as a schematic top view (3, third column) and side view (4, fourth column) of the wurtzite (1120) [frames labeled (a), first row] and (1010) (b) cleavage surfaces of CdSe (second row) and the cubic GaAs(110) surface [frames (c), third row]. The filled and empty ellipses in the fourth column represent a filled and an empty dangling bond, respectively. The tunneling voltages used for measuring the images are indicated in the lower right corner of each STM image. The tunnel current was 0.2 nA.

wide). The best images were measured in the voltage ranges -2 to -3.5 V and $+1$ to $+2.5$ V. Since the CdSe samples were *n* doped, the occupied state images (measured at negative voltages) show an occupied surface state or resonance at the top of the valence band [valence-band maximum (VBM)]. The voltage range in which good STM images can be obtained gives an indication about the width of the dispersion of the uppermost occupied surface state or resonance. If band bending effects are taken into account,[11] one can estimate that the occupied surface state has a width of about 1 eV. Similarly, the empty state images arise from an empty state or resonance about 0.5–1.5 eV above the conduction-band minimum (CBM). No indications were found that more states contribute to the STM images, although this cannot be excluded.

Figure 2 shows an atomically resolved image of the occupied and empty states of the CdS(1010) surface. The surface structure closely resembles that observed for CdSe(1010) [see Fig. 1(b)]. Again it was not possible to extract a stable tunnel current within the band gap. We have not been able to detect any difference between the two materials so far.

We also observed large elevations of bright contrast (Fig. 3) with a diameter of 4–5 nm. These elevations superposed the atomic-scale contrast of the clean surface. These localized areas appear as elevations in the occupied and empty state images (both polarities of the tunneling voltage). The contrast is consistent with the scanning tunneling microscope imaging of a downward potential surrounding a localized positive charge.[12] We thus attribute these charges to surface and subsurface In dopant atoms in analogy to dopant atoms observed by STM in (110) surfaces of a variety of III-V semiconductors.[2–4,10,12–14]

IV. DISCUSSION

A. 1×1 reconstruction

The determination of the dimensions of the surface unit cell from the STM images allows us to establish that both surfaces (1120) and (1010) exhibit a 1×1 reconstruction because the respective unit cells on bulk planes have, within the error margin, the same sizes. This result confirms previous results deduced from low-energy electron diffraction[15–19] (LEED) and low-energy positron diffraction

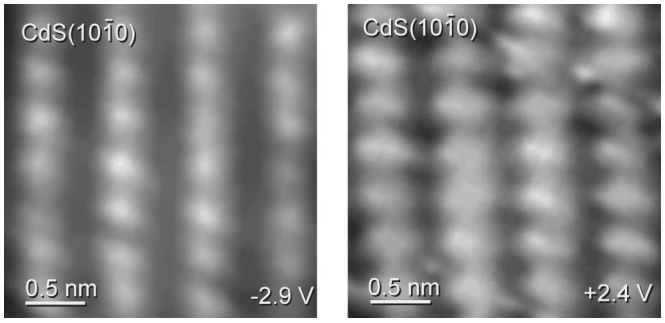

FIG. 2. (a) Occupied and (b) empty state images of the CdS (1010) surface. The images were measured at -2.9 and $+2.4$ V, respectively (tunnel current 0.3 nA).

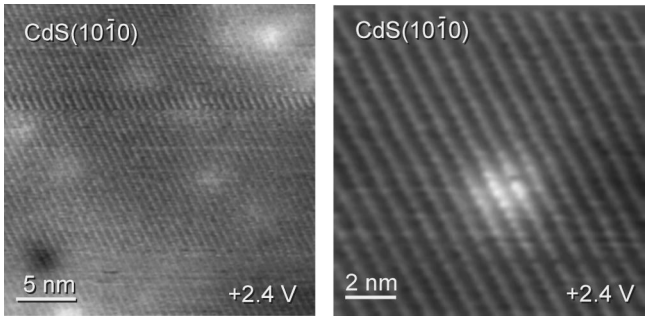

FIG. 3. Constant current image of the CdS $(10\bar{1}0)$ surface showing large elevations appearing bright in this gray scale representation. The elevations are the signature of the positively charged In dopant atoms in different subsurface layers. The right-hand frame shows a dopant atom at a higher magnification.

measurements,[17,18,20] as well as theoretical calculations[21] of wurtzite compound semiconductor cleavage surfaces. In addition, the STM images exclude the existence of other minority surface reconstructions.

B. Electronic structure of the $(10\bar{1}0)$ surfaces

At this stage we discuss which surface states or resonances give rise to the atomic contrast observed in the STM images. The frames denoted by the numbers 3 and 4 in Fig. 1 show schematic drawings of the atomic surface structure as determined by LEED.[19] A comparison with the STM images reveals that at one polarity only half as many maxima occur in each STM image as atoms present in a unit cell. Thus either two atoms give rise to one surface state or resonance or only every second atom has a state that can be imaged by STM at one polarity. First we turn to photoemission results. Photoemission measurements of the CdSe and CdS (1010) surfaces indicate that these surfaces both have one occupied surface state or resonance close to the top of the valence band.[22] The state exhibits a relatively weak dispersion (about 1 eV wide) and a maximum at the $\bar{\Gamma}$ point of the surface Brillouin zone (about 0.2 and 0.4 eV below the VBM for CdS and CdSe, respectively). Its minimum in energy is at the edge of the Brillouin zone (about 1.4 eV below the VBM). The energy of this state agrees well with the voltages of the STM images. This suggests that the state observed by photoemission corresponds to the one observed in the STM images of Figs. 1(b1) and 2(a), i.e., the STM images show the spatial distribution of the state above the surface, whereas the photoemission probes the dispersion. However, photoemission does not provide us with a detailed microscopic picture, i.e., the origin of the feature remains unknown.

The next step is thus a comparison of our data with electronic-structure calculations of the cleavage surfaces of II-VI semiconductors.[23–28] We will discuss the results independently of the specific material because the number of theoretical results is limited. Most of the results focus on the specific systems investigated here anyway, and we did not observe any difference between CdSe and CdS by STM. The theoretical results show that the different materials all have a similar electronic structure, only the band gap changes. The calculations of $(10\bar{1}0)$ surfaces predict between one and three occupied surface states close to the valence-band maximum. These surface states and resonances are labeled A_4, A_5, and A_6,[23] P_1 and P_3,[24] S_1, S_2, and (in some cases) S_5,[25–27] or S_3.[28] The energetic location makes all these states prospective candidates for the state observed by photoemission and STM. Other surface states far away from the band gap cannot be imaged by STM and will not be discussed here. The surface states found close to the band edge can be distinguished according to their properties.

(i) The state referred to as (Ref. 25–27) consists primarily of a p_z component localized at the top-layer anion and a p_x component at the second-layer cation. The same result is found for the A_5. (Fig. 15 in Ref. 23) or P_1 (Fig. 5 in Ref. 24) state: This state has a typical *dangling-bond character and are localized above the surface anion* (here the Se atoms). The dangling bond extends quite far into the vacuum. It has an analog on the GaAs(110) surface,[29,30] where the occupied dangling bond above the As atoms almost entirely dominates the STM images obtained at negative voltages, leading to STM images like that shown in Fig. 1(c1).

(ii) The S_2 state has an energy below the S_1 state and is mainly localized on the second layer close to the cation. It may be viewed as a back bond state. Since its main localization is in the second layer, it is unlikely to contribute significantly to the tunnel current. The corresponding state on InP(110) surfaces contributes only little to the STM images and only at large negative voltages.[30]

(iii) The A_4,[23] S_3,[25] or P_3 (Ref. 24) state has a density of states localized between the top-layer anion and cation. This state is best described as a bridge bond. It would lead to two maxima in the density of states along the [0001] direction next to a Se atom in the surface layer. This is not observed; hence this state is not imaged in the STM images.

Of the states discussed above only the dangling-bond state (i) contributes significantly to the STM images because it extends far into the vacuum, has the correct number of maxima per unit cell, and has an energy close to the valence-band maximum, which already allows electrons to tunnel from the dangling-bond state into the tip at small voltages (as observed experimentally). Furthermore, it is possible to conclude that the electrons tunnel from the $\bar{\Gamma}$ point of the surface Brillouin zone into the tip because the exponential energy dependence of the transfer coefficient favors states closer to the valence-band maximum. At the $\bar{\Gamma}$ point the dangling-bond band is closest to the VBM and a surface resonance. Thus the STM images of the occupied states on the (1010) surface show the lateral distribution above the surface of the dangling-bond resonance close to the $\bar{\Gamma}$ point. This result is also corroborated by a calculation of the wurtzite GaN (1010) surface.[31]

The interpretation of the empty states is complicated due to the lack of an inverse photoemission study of wurtzite cleavage surfaces. Thus we have to rely entirely on theoretical results. Wang and Duke show the dispersion of an empty surface resonance for ZnO,[26] CdS,[27] and CdSe (Ref. 27) (1010) surfaces about 1 eV above the CBM. However, Pollmann *et al.*[23] and Schröer, Krüger, and Pollmann[24] find a similar empty surface state or resonance for CdS about 2–3

eV above the CBM (denoted C_3 in Ref. 23 and S_3 in Ref. 24). The latter energy would be too high above the CBM to account for the features observed in the STM images (we find only the empty surface state at lower energy). A solution to this problem may be that the minimum of the empty surface state is resonant with the conduction band at the Γ point and close to the band edge, as predicted by Wang and Duke.[26,27]

Schröer, Krüger, and Pollmann show that the empty surface state is localized at the surface anion and cation. In principle, the STM should thus image maxima of the empty states at anions and cations simultaneously. This is not observed; hence the measurements suggest that one part of this state must decay faster into the vacuum than the other one. A comparable situation exists on InP(110):[30] the empty dangling bond has a noticeable density of states above the anion, which decays faster in favor of the density of states localized above the cation. Thus at larger distances, where the STM probes the density of states, only one maximum above the cation can be observed. Such a situation may exist on wurtzite surfaces too. This is corroborated by the distribution of the density of states at the anion: In Fig. 5 of Ref. 24 the empty density of states has two maxima close to the anion, also leading to two maxima in the STM images per unit cell. This is not observed, although the resolution was sufficient to be able to observe this effect in principle. Thus the anionic part of this state is likely to decay faster. In addition, the label C_3 of this state[23] clearly indicates its primarily cationic character, i.e., the empty resonance is mainly localized near the cation. A direct experimental test of the relative location of the empty state maxima toward the occupied density of states maxima was not possible because the tip becomes easily unstable on the weakly bonded CdSe and CdS surfaces. From the above discussion we conclude that the STM images of the empty states of the (1010) surfaces show an empty dangling-bond resonance in the center of the surface Brillouin zone. Electronic-structure calculation of GaN (1010) supports our result.[31]

C. Electronic structure of the $(11\bar{2}0)$ surfaces

Theoretical calculations of $(11\bar{2}0)$ surfaces yield a very similar band structure compared to the (1010) surfaces, but fewer data have been published as yet. All theoretical data concern the occupied states. Two states are found on ZnO (Ref. 26) and CdSe (1120).[25] Only one state is predicted for wurtzite ZnSe (1120) (Ref. 28) close to the VBM.

(i) The state referred to as S_1 (Ref. 26) (and S_3 in Ref. 28) consists primarily of a p_z component of the top-layer anion and a p_x component of the second-layer cation. The energy of this state is 0.5–1.5 eV below the VBM. Its maximum and minimum are in the center and at the edge of the Brillouin zone, respectively. All these properties are in analogy to the occupied dangling-bond state on (1010) surfaces (see above). Thus, on (1120) surfaces the corresponding occupied state is also likely to be the dangling-bond state localized above the anion (Se atoms) in the surface layer.

(ii) The S_2 state has an energy below the S_1 state[26] and is mainly localized on the second layer. It may be viewed again as a back bond. Since its main localization is in the second layer, it is unlikely to contribute significantly to the tunnel current. Therefore, the STM images of the occupied density of states show mainly an anion-derived dangling bond.

The situation of the empty states is less clear. Only the dispersion of the empty state is imaged without further discussion. The dispersion has some similarities to the empty dangling-bond band on (1010) surfaces. Thus we tentatively suggest that the STM images show an empty dangling-bond state.

The result that the STM probes the anion- and cation-derived dangling-bond states is corroborated by the fact that the (1120) surface has a bonding geometry closely related to that of the, e.g., GaAs(110) surface: Each surface atom has one bond to a second-layer atom and two bonds within the surface atomic chain. In fact, the structure of the (1120) surface corresponds exactly to the structure of a stacking fault exposed on a (110) surface. Stacking faults connected to partial dislocations penetrating through a GaAs(110) surface can be found in Figs. 3 of Refs. 32 and 33. The zigzag chain visible in the high-resolution images of a stacking fault (Fig. 3 in Ref. 32) is the signature of the abab stacking of the local wurtzite structure (see also the indication of the stacking in Fig. 3 of Ref. 33). The abcabc stacking of the (111) planes in the cubic phase is indicated in Fig. 1 for comparison. Thus the stacking fault exhibits exactly the same zigzag pattern as that observed on the CdSe (1120) surface. In addition, the maxima in the stacking fault area have nearly the same height and shape as the dangling bonds imaged on defect-free (110) surfaces. In conjunction with the knowledge that the dangling bonds dominate the contrast of the STM image of the GaAs(110) surfaces,[29,30] we conclude that the image features in the stacking fault arise from a dangling bond too. The overlap of the maxima in the STM image with the positions of the anions in the structural model (Fig. 4 of Ref. 33) supports this conclusion. This further backs the existence of an occupied dangling bond above the anions on the wurtzite structure (1120) cleavage surfaces.

D. Effect of buckling on the STM images

The buckling of the surface bonds on (110) surfaces is known to induce a lateral movement of the maxima of the density of states above the anions and cations. This lateral shift was quantified for GaAs(110) and directly correlated to the buckling via an electronic structure calculation.[29] A similar effect can be expected to occur on wurtzite surfaces as well. On (1010) cleavage surfaces the shift is a relative shift between the occupied and empty state images in direct analogy to the (110) surfaces. On (1120) surfaces the shift also affects the width of the zigzag chain. This allows us to determine the shift from one image thus increasing the accuracy. We obtained a width of the zigzag chains of 0.23 $\pm$0.01 nm. The value is larger that the ideal bulk separation of the atoms (0.215 nm). In principle, it should even be possible to measure the shifts of the anions and cations separately because of the symmetry of the atomic chains. However, a more detailed analysis requires electronic-structure calculations not available so far.

E. Suitability of the cleavage surfaces for defect studies

A STM investigation of bulk point defects requires that (i) the surface must be produced by cleavage in order to avoid

any changes by thermal cleaning procedures and the cleavage surface should be preferentially perpendicular to the growth direction of interest (in order to allow a real cross-sectional view), (ii) the surface should have a 1×1 reconstruction because a dimerization would already obscure the point defects, (iii) the electronic structure should allow an atom-selective imaging by STM in order to distinguish between defects on the anion and cation sublattice, and (iv) the charges of defects should be identifiable even for subsurface defects. The investigated surfaces have all these properties. (i) and (ii) are fulfilled by the wurtzite cleavage surfaces as discussed above. An atom-selective imaging is possible because a charge transfer from the cations to the anions in the surface layer occurs and yields a completely filled state localized at the anion and an empty state at the cation (see schematic side views in Fig. 1). The dangling-bond states are pushed out of the fundamental band gap and thus the surfaces are unpinned. The dangling-bond states have been found to dominate the contrast of the STM image and therefore the STM images of all three cleavage surfaces are chemically sensitive,[29] i.e., anions and cations are separately imaged. The combination of properties (i)–(iii) in general makes the observation of charged subsurface defects possible (iv) because on an unpinned surface the shallow band bending arising from localized charges is not obscured. The direct observation of the charged dopant atoms in different subsurface layers (Fig. 3) further corroborates the result that no surface states are within the band gap and the surface is unpinned. We can thus conclude that most properties of the wurtzite cleavage surface are analogous to those of (110) cleavage surfaces of cubic compound semiconductors and the cleavage surfaces investigated here are suitable for bulk defect investigations by STM.

V. CONCLUSION

In conclusion, we present atomically resolved STM investigation of cleavage surfaces of II–VI compound semiconductors with a wurtzite structure. The analysis of the images confirmed the 1×1 reconstruction on both the (1120) and (1010) cleavage surfaces of CdSe and CdS. The image features can be attributed in the occupied and empty state images to the completely filled and empty dangling bonds above the anions and cations, respectively. This is the signature of a charge transfer from anions to cations in analogy to, e.g., GaAs(110) surfaces. Thus the STM images are chemically sensitive. No states in the band gap were observed. It was possible to observe charged dopant atoms. We conclude that the two cleavage surfaces studied are suitable for cross-sectional investigations of heterostructures as well as point defects.

ACKNOWLEDGMENT

The authors would like to express their thanks to K. H. Graf for technical support.

[1] R. M. Feenstra, J. M. Woodall, and G. D. Petit, Phys. Rev. Lett. **71**, 1176 (1993).
[2] M. B. Johnson, O. Albrektsen, R. M. Feenstra, and H. W. M. Salemink, Appl. Phys. Lett. **63**, 2923 (1993); **64**, 1454 (1994).
[3] J. F. Zheng, M. B. Salmeron, and E. R. Weber, Appl. Phys. Lett. **64**, 1836 (1994); **65**, 790 (1994).
[4] C. Domke, Ph. Ebert, M. Heinrich, and K. Urban, Phys. Rev. B **54**, 10 288 (1996).
[5] O. Albrektsen, D. J. Arent, H. P. Meier, and H. W. M. Salemink, Appl. Phys. Lett. **57**, 31 (1990).
[6] S. Gwo, K.-J. Chao, C. K. Shih, K. Sadra, and B. G. Streetman, Phys. Rev. Lett. **71**, 1883 (1993).
[7] J. F. Zheng, J. D. Walker, M. B. Salmeron, and E. R. Weber, Phys. Rev. Lett. **72**, 2414 (1994).
[8] M. Pfister, M. B. Johnson, S. F. Alvarado, H. W. M. Salemink, U. Marti, D. Martin, F. Morrier-Genoud, and F. K. Reinhart, Appl. Phys. Lett. **65**, 1168 (1994).
[9] R. M. Feenstra, D. A. Collins, D. Z.-Y. Ting, M. W. Wang, and T. C. McGill, J. Vac. Sci. Technol. B **12**, 2592 (1994).
[10] M. B. Johnson, P. M. Koenraad, W. C. van der Vleuten, H. W. M. Salemink, and J. H. Wolter, Phys. Rev. Lett. **75**, 1606 (1995).
[11] R. M. Feenstra and J. A. Stroscio, J. Vac. Sci. Technol. B **5**, 923 (1987).
[12] J. F. Zheng, X. Liu, N. Newman, E. R. Weber, D. F. Ogletree, and M. Salmeron, Phys. Rev. Lett. **72**, 1490 (1994).
[13] M. B. Johnson, H. P. Meier, and H. W. M. Salemink, Appl. Phys. Lett. **63**, 3636 (1993).
[14] Ph. Ebert, M. Heinrich, M. Simon, C. Domke, K. Urban, C. K. Shih, M. B. Webb, and M. G. Lagally, Phys. Rev. B **53**, 4580 (1996).
[15] C. B. Duke, A. Paton, Y. R. Wang, K. Stiles, and A. Kahn, Surf. Sci. **197**, 11 (1988).
[16] A. Kahn, C. B. Duke, and Y. R. Wang, Phys. Rev. B **44**, 5606 (1991).
[17] T. N. Horsky, G. R. Brandes, K. F. Canter, C. B. Duke, A. Paton, D. L. Lessor, A. Kahn, S. F. Horng, K. Stevens, K. Stiles, and A. P. Mills, Jr., Phys. Rev. B **46**, 7011 (1992).
[18] T. N. Horsky, G. R. Brandes, K. F. Canter, C. B. Duke, S. F. Horng, A. Kahn, D. L. Lessor, A. P. Mills, Jr., A. Paton, K. Stevens, and K. Stiles, Phys. Rev. Lett. **62**, 1876 (1989).
[19] C. B. Duke, Chem. Rev. **96**, 1237 (1996).
[20] C. B. Duke, D. L. Lessor, T. N. Horsky, G. R. Brandes, K. F. Canter, P. H. Lippel, A. P. Mills, Jr., A. Paton, and Y. R. Wang, J. Vac. Sci. Technol. A **7**, 2030 (1989).
[21] C. B. Duke and Y. R. Wang, J. Vac. Sci. Technol. A **6**, 692 (1988).
[22] K. O. Magnusson and S. A. Flodström, Phys. Rev. B **38**, 6137 (1988).
[23] J. Pollmann, P. Krüger, M. Rohlfing, S. Sabisch, and D. Vogel Appl. Surf. Sci. **104/105**, 1 (1996).
[24] P. Schröer, P. Krüger, and J. Pollmann, Phys. Rev. B **49**, 17 092 (1994).
[25] Y. R. Wang, C. B. Duke, K. Stevens, A. Kahn, K. O. Magnusson, and S. A. Flodström, Surf. Sci. Lett. **206**, L817 (1988).
[26] Y. R. Wang and C. B. Duke, Surf. Sci. **192**, 309 (1987).
[27] C. B. Duke and Y. R. Wang, J. Vac. Sci. Technol. B **6**, 1440

(1988).
[28] Y. R. Wang, C. B. Duke, and C. Mailhiot, Surf. Sci. Lett. **188**, L708 (1987).
[29] R. M. Feenstra, J. A. Stroscio, J. Tersoff, and A. P. Fein, Phys. Rev. Lett. **58**, 1192 (1987).
[30] Ph. Ebert, B. Engels, P. Richard, K. Schroeder, S. Blügel, C. Domke, M. Heinrich, and K. Urban, Phys. Rev. Lett. **77**, 2997 (1996).
[31] J. E. Northrup and J. Neugebauer, Phys. Rev. B **53**, 10 477 (1996).
[32] G. Cox, D. Szynka, U. Poppe, K. H. Graf, K. Urban, C. Kisielowski-Kemmerich, J. Krüger, and H. Alexander, Phys. Rev. Lett. **64**, 2402 (1990).
[33] G. Cox, D. Szynka, U. Poppe, K. H. Graf, K. Urban, C. Kisielowski-Kemmerich, J. Krüger, and H. Alexander, J. Vac. Sci. Technol. B **9**, 726 (1991).